

## Global description of EUSO-BALLOON instrument

C. MORETTO<sup>1</sup>, S. DAGORET-CAMPAGNE<sup>1</sup>, J.H. ADAMS<sup>19</sup>, P. VON BALLMOOS<sup>2</sup>, P. BARRILLON<sup>1</sup>, J. BAYER<sup>5</sup>, M. BERTAINA<sup>12</sup>, S. BLIN-BONDIL<sup>1</sup>, F. CAFAGNA<sup>7</sup>, M. CASOLINO<sup>13,10,11</sup>, C. CATALANO<sup>2</sup>, P. DANTO<sup>4</sup>, A. EBERSOLDT<sup>6</sup>, T. EBISUZAKI<sup>13</sup>, J. EVRARD<sup>4</sup>, PH. GORODETZKY<sup>3</sup>, A. HAUNGS<sup>6</sup>, A. JUNG<sup>14</sup>, Y. KAWASAKI<sup>13</sup>, H. LIM<sup>14</sup>, G. MEDINA-TANCO<sup>15</sup>, H. MIYAMOTO<sup>1</sup>, D. MONNIER-RAGAIGNE<sup>1</sup>, T. OMORI<sup>13</sup>, G. OSTERIA<sup>9</sup>, E. PARIZOT<sup>3</sup>, I.H. PARK<sup>14</sup>, P. PICOZZA<sup>13,10,11</sup>, G. PRÉVÔT<sup>3</sup>, H. PRIETO<sup>13,17</sup>, M. RICCI<sup>8</sup>, M.D. RODRIGUEZ FRIAS<sup>17</sup>, A. SANTANGELO<sup>5</sup>, J. SZABELSKI<sup>16</sup>, Y. TAKIZAWA<sup>13</sup>, K. TSUNO<sup>13</sup> FOR THE JEM-EUSO COLLABORATION<sup>19</sup>.

<sup>1</sup> *Laboratoire de l'Accélérateur Linéaire, Univ Paris Sud-11, CNRS/IN2P3, Orsay, France*

<sup>2</sup> *Institut de Recherche en Astrophysique et Planétologie, Toulouse, France*

<sup>3</sup> *AstroParticule et Cosmologie, Univ Paris Diderot, CNRS/IN2P3, Paris, France*

<sup>4</sup> *Centre National d'Études Spatiales, Centre Spatial de Toulouse, France*

<sup>5</sup> *Institute for Astronomy and Astrophysics, Kepler Center, University of Tübingen, Germany*

<sup>6</sup> *Karlsruhe Institute of Technology (KIT), Germany*

<sup>7</sup> *Istituto Nazionale di Fisica Nucleare - Sezione di Bari, Italy*

<sup>8</sup> *Istituto Nazionale di Fisica Nucleare - Laboratori Nazionali di Frascati, Italy*

<sup>9</sup> *Istituto Nazionale di Fisica Nucleare - Sezione di Napoli, Italy*

<sup>10</sup> *Istituto Nazionale di Fisica Nucleare - Sezione di Roma Tor Vergata, Italy*

<sup>11</sup> *Università di Roma Tor Vergata - Dipartimento di Fisica, Roma, Italy*

<sup>12</sup> *Dipartimento di Fisica dell'Università di Torino and INFN Torino, Torino, Italy*

<sup>13</sup> *RIKEN Advanced Science Institute, Wako, Japan*

<sup>14</sup> *Sungkyunkwan University, Suwon-si, Kyung-gi-do, Republic of Korea*

<sup>15</sup> *Universidad Nacional Autónoma de México (UNAM), Mexico*

<sup>16</sup> *National Centre for Nuclear Research, Lodz, Poland*

<sup>17</sup> *Universidad de Alcalá (UAH), Madrid, Spain*

<sup>18</sup> *University of Alabama in Huntsville, Huntsville, USA*

<sup>19</sup> <http://jemeuso.riken.jp>

*moretto@lal.in2p3.fr*

**Abstract:** EUSO-Balloon is a pathfinder prefiguring the future fluorescence space telescope JEM-EUSO that should be installed on-board the International Space Station before the end of this decade. This telescope will be the payload of a stratospheric balloon operated by CNES, starting its flight campaign in 2014. Current technical developments for JEM-EUSO have been implemented in EUSO-Balloon. The complete design of this instrument is presented. It consists of an advanced telescope structure, including a set of three Fresnel lenses having an excellent focusing performance onto its pixelized UV Camera. All the stages of the signal processing are reviewed from the photodetector, the analog electronics producing the digitised data, and also the triggers selecting the events while rejecting the random background, the acquisition system allowing the data storage and the monitoring permitting the instrument control during operation. The key parameters of the instrument are presented and their chosen value motivated.

**Keywords:** JEM-EUSO, UHECR, space instrument, balloon experiment, instrumentation

## 1 Introduction

EUSO-Balloon is a telescope aiming at verifying the conceptual design as well as the technologies foreseen to be applied for the construction of the future space telescope JEM-EUSO [1]. Even if this instrument is a reduced version of JEM-EUSO, it however includes almost all the required components of the original space mission. The scientific and technical goals of its mission are reviewed in [2]. The physical performances if the instrument are estimated in [3]. This instrument will be the payload of a stratospheric balloon operated by CNES, to perform a series of night-flights at altitudes of 40 km, at various earth locations, lasting from a few hours to tens of hours. This program requires payload recovery after landing either in water or hard soil, and repairing after each mission. The special atmospheric environmental conditions and recovery requirements involve

much precautions in the design and imply dedicated tests with the realisation of prototypes.

This paper is organised as follows. First, section 2 gives the overview of the instrument, including its particular mechanical design adapted to the balloon flights. Section 3 provides details on the subsystems and highlights reasons for the chosen design. Afterward, the section 4 deals with the series of preliminary measurements and tests which are mandatory before the commissioning of the instrument for exploration. Finally, the control and analysis tasks to be performed during the operation are mentioned in section 5.

## 2 The Instrument overview

The EUSO-balloon instrument structure is shown in the figure 1 and its main characteristics are given in the table 1.

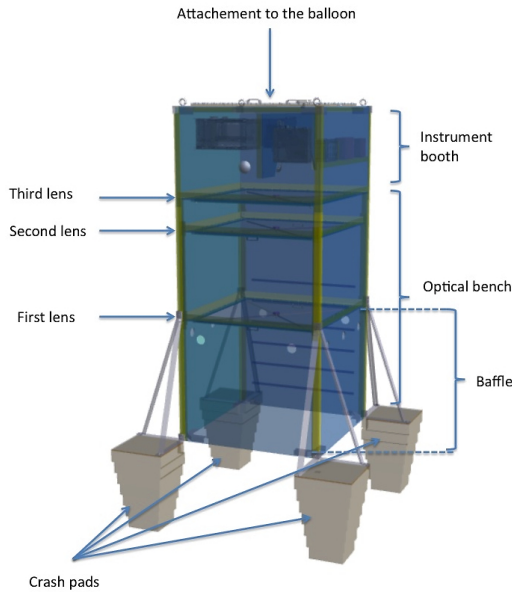


**Fig. 1:** EUSO-Balloon Instrument Overview.

These parameters will be justified in the section 3 devoted to the subsystems. This parallelepiped-shaped telescope presents a wide field of view of  $12^\circ \times 12^\circ$  for a collecting surface of  $1 \text{ m} \times 1 \text{ m}$ . It points to the nadir direction toward the earth. It basically consists in an optical bench associated to an instrument booth placed at the focal position. The optical bench comprises two lenses. The instrument booth includes the whole electronics inside a pressurised watertight box. One side of the instrument booth is provided by the third lens. The instrument includes an external roof-rack permitting the fixation of complementary instruments like an infra-red camera for atmosphere monitoring.

### 2.1 General characteristics and functions

The optical subsystem includes the optical bench which have the purpose of focusing parallel light rays in a narrow focal point on a pixelized surface, consisting in an array of photodetectors called MAPMTs (Multi-Anode Photomultipliers). This Focal Surface (FS) is instrumented by an electronics which has the properties of a very high sensitivity in the UV range, fast measurement rate within the microsecond time scale, auto-triggering capability, event filtering and event recording. This electronics is capable to record on disk a burst of 128 consecutive sky pictures separated each-other by a Gate Time Unit (GTU) of  $2.5 \mu\text{s}$ .

### 2.2 Instrument structure

The mechanics of the instrument is made of Fibrelam® panels, arranged together through fibreglass sections. The instrument is coated by an insulating cover to protect the instrument's components from fast temperature changes during balloon ascent and descent. Special watertight valves inserted in the optical bench are used to enable pressure equilibrium with the external environment. Wherever the after-flight landing location occurs, the instrument must be recovered with the smallest damages. The bottom part is equipped with crash-pads which absorb brutal deceleration (up to 15 G) when landing on ground. A baffle with special holes in the optical bench are used as a piston-effect to damp the shock for a fall over water. The instrument booth

General parameters	
Field of view	$12^\circ \times 12^\circ$
Aperture	$1 \text{ m} \times 1 \text{ m}$
Optics	
Focal Length	1.62 m
Focal Point Spread (RMS)	2.6 mm
Focal Surface	
Curvature Radius	2.5 m
Number of Pixels	2304
Pixel field of view	$0.25^\circ \times 0.25^\circ$
Pixel size	$2.88 \text{ mm} \times 2.88 \text{ mm}$
BG3 UV Filter transmittance	98 %
Wavelength range	290 nm - 430 nm
Number of MAPMTs	$6 \times 6$
PhotoDetection (MAPMTs)	
Number of channels	64
Photo detection efficiency	$\sim 35 \%$
Gain	$10^6$
Pulse duration	2 ns
Two pulses separation	5 ns
Dynamic Range	$\sim 1 - 1000 \text{ photons}/\mu\text{s}$
Maximum tube current	$100 \mu\text{A}$
Signal Measurement (ASIC)	
Photon Counting (64 ch), photoelectrons	0.3 pe (50 fC) - 30 pe (5 pC)
Charge to Time Conv (8 ch)	2 pC (10 pe) - 200 pC (100 pe)
Shapping time	30 ns
Sampling period (GTU)	$2.5 \mu\text{s}$
Readout Clock	40 MHz
Triggers (FPGA, Virtex 6 (L1) and Virtex 4 (L2))	
L1 rate	7 Hz (1-100 Hz)
L2 rate	Max 50 Hz
Event readout and DAQ (CPU, Clocks, GPS)	
Event size	330 kB
Data flow	3.24 Mb/s
Readout Clock	40 MHz
Event dating	at $\mu\text{s}$ level

**Table 1:** Typical parameters of the instrument

which is a totally watertight sealed box, consists of a central aluminium plate on which the various electronic boxes are fixed. One of its side is the third lens. The opposite one is an aluminium radiator used to dissipate the heat generated by electronics equipments. The instrument is surrounded by buoys to avoid sinking in case of splashdown and to raise straight up the instrument booth above the water level.

## 3 The Instrument subsystems

The instrument is broken down into subsystems defined to be the optics, the Focal Surface (FS), the photodetector with the MAPMTs, the signal measurement with the ASICs, the trigger readout with the Photo-Detector Module Board (PDMB) and the Cluster Control Board (CCB). The Data Acquisition System (DAQ) and the utilities like the monitoring also called the House-Keeping (HK) and the power supplies. Those subsystems are all described below.

### 3.1 Optics subsystem

The optics subsystem involves three lenses. Its goal is to provide the best focusing for the smallest focal distance. The focusing requirement is constrained by the pixel size of the photodetection system. Due to the wide angular field of view, it is necessary to combine 3 flat lenses. External ones are focusing one-sided Fresnel lens and the middle one is purely dispersive to correct for chromatic aberrations. These lenses are manufactured in PMMA material [4]. The ray tracing calculations including the temperature profile expected for flights in cold and warm cases provide a focal length of 1.62 m and a focal point spread width of the order of 2.6 mm, smaller than the pixel size.

### 3.2 Front-End Electronics

MAPMTs constituting the FS, provide anode signals measured and digitised by ASICs, themselves readout by FPGA to run the trigger algorithm. The FS is arranged into a so-called Photo-Detector Module (PDM) whose design and effective realisation is described in details in [5]. We review in the following the main properties of this electronics.

**Focal Surface** The focal surface is a slightly curved surface, similarly to that of the JEM-EUSO central PDM. It is an array of  $48 \times 48$  pixels of  $2.88 \text{ mm} \times 2.88 \text{ mm}$  size exceeding slightly the focal point spread. Practically, the focal surface of the PDM is broken up into a set of 9 identical Elementary Cells (ECs), which are matrices of  $2 \times 2$  MAPMTs. The photocathode is covered by a BG3 UV filter. Inside the PDM structure, the 9 ECs are disposed and tilted according to the appropriate shape required for the FS.

**MAPMTs** They are photon detectors consisting of a matrix of  $8 \times 8$  pixels. Each pixel is associated to an anode generating a charge or a current in output. Their sensitivity is as low as a few tenths of photon and their dynamic range can extend up to few thousands photon per  $\mu\text{s}$  when working at their nominal high gain,  $10^6$ .

**High voltage power supply** MAPMTs require to be polarised with 14 high voltages. The latter are generated by a high voltage power supply (Cockroft-Walton (CW) type to restrain the power consumption). The nominal high voltage of the photocathode is  $-900 \text{ V}$  for a MAPMT nominal gain at  $10^6$ . The effective dynamic range can be extended up to  $10^7$  photons/ $\mu\text{s}$  by reducing gradually the gain down to 30. Fast switches (SW) responsive at  $\mu\text{s}$  timescale, adapt HV values to tune the MAPMT gain according to the intensity of photon flux. Because a large photon flux generating anode current above  $100 \mu\text{A}$  would destroy the tube, this automatic control system can even switch off the gain. Practically this switching decision logic is implemented in a FPGA reading out the ASICs. In the PDM, there is 9 independent CW with their individual 9 SW, assembled into two separated HVPS boxes, each CW controlling independently the 9 ECs High Voltages.

**ASICs** 36 SPACIROC [6] type ASICs are used to perform the anode signals measurement and digitisation of the 36 MAPMTs. These ASICs have 64 channels. Their analog inputs are DC-coupled to the MAPMT anodes. They process the 64 analog signals in parallel in two modes : 1) in photoelectron counting mode, in a range from 1/3 of photoelectrons up to 100 photoelectrons, by discriminating over a programmed threshold each of the channels, 2) by estimating the charge from 20 pC to 200 pC, by time over threshold determination for exclusive groups of 8 anodes current sums from clusters of 8 contiguous pixels. The 64 analog channels are balanced each-other relatively by gain matching over 8-bits. The discrimination voltage level used in the photon-counting is provided by a 10-bit DAC (Digital to Amplitude converter). In both cases the digitisation is performed by 8-bits counters every GTU. There is no data buffering on the ASIC. The data are transferred to the FPGA each GTU under the sequencing frequency of a 40MHz clock.

**Trigger** The Instrument includes two trigger stages. The level 1 trigger (L1) implemented in the FPGA (Xilinx Virtex 6) of a PDM-Board (PDMB), belonging to the Front-End Electronics. The PDMB readouts the data from the 36 ASICs into its internal memory (the event buffer) each GTU to compute the L1 trigger. Its principle consists in counting an excess of signals over background in groups of  $3 \times 3$  pixels lasting more than a preset persistence time. The background rate seen by pixel is monitored continuously to adjust in real-time the trigger threshold which is adjusted such as the L1 rate is kept at a fixed level of a few Hz compatible with the DAQ recording rate. The trigger is evaluated each GTU. Because Air-Showers may extend over 100 GTU, this trigger has the buffering capability over 128 consecutive GTU. To reduce the dead-time induced by event readout, the event buffer is doubled.

### 3.3 Data acquisition

The data acquisition system is part of the computing system DP (Data Processing). It comprises the CCB designed to produce the second level trigger L2, which is described in [7]. For each generated L1 trigger, the CCB reads the data corresponding to the 128 consecutive GTU from the PDMB buffer. In JEM-EUSO, the CCB is devoted to the combination of 9-PDMB triggers and to reduce the resulting combined trigger rate to about a few Hz or less compatible with the data storage capabilities of the DAQ. The triggering role of the CCB in EUSO-Balloon is marginal as there is only one PDM. However it has the task to read the whole event from the Front-End and to pass it to the CPU. The L2 decision is propagated to the Clock-Board (CLKB, based on a Xilinx Virtex5 FPGA) generating all the clocks used by the electronics, itself associated with a GPS-Board to provide the event time tagging data with an accuracy of a few microseconds. The CPU (Motherboard iTX-i2705 model, processor Atom N270 1.6 GHz) merges the event data with the time tagging data to build an event of a size of 330 kB, leading to a data flow of 3MB/s for a 10 Hz L1-L2 trigger. The CPU write all the data on disks (1 TB CZ Octane SATA II 2.5 SSD) and may also send to telemetry a subset of flagged events by CCB for event monitoring.

### 3.4 Monitoring

The instrument behaviour is controlled at low frequency by the House-Keeping system (HK) which is a part of DP. It is based on a commercial micro controller board (Arduino Mega 2560) designed to control temperatures, voltages, and alarms raised by several boards. The CPU poll from time to time the alarms and initiate corresponding foreseen actions. HK is connected to the telemetry system to receive basic commands namely those that allow to turn on-off most of the boards power supplies through relays.

### 3.5 Power supply and electrical architecture

The instrument runs autonomously thanks to a set of 60 battery cells providing 28 V (225 W during 24 H) to a set of Low-Voltage boards generating isolated-decoupled lower voltages to the PDM (HVPS and PDMB), DP (CPU,CLKB,GPSB,CCB and HK). The electrical architecture follows the EMC rules to prevent floating reference voltages induced by bad grounding (current ground loop effect).



## 4 Assembly and tests

After fabrication, the subsystems directly related to the physics measurements need to be calibrated in an absolute way. The goal of the absolute calibration is to relate a measured digitised signal into the true number of photons impinging on the Focal Surface or on the first lens. Thus the Optics and the photodetection done by the MAPMTs will be calibrated. Other subsystems like the trigger has to be tested once the instrument is close to final assembly. Each of the subsystems of the instrument are calibrated if necessary and tested before the full integration. Then the assembled instrument is then tested entirely.

### 4.1 The optical tests

Even if the focal length of each lens and the combined focal length can be predicted by calculation, the real values resulting from the machining are poorly known, only at a few tens of centimetres accuracy. This is not enough to achieve a resolution smaller than the pixel size. Thus the relative distance between the three lenses and the Focal Surface has to be measured experimentally by using a large parallel UV beam along optical axis, sent over the first lens and measuring the Focal Length by adjusting the position of a CCD camera to get its position obtained for the narrowest focused spot.

### 4.2 Measuring the MAPMT performances

Each channel of the MAPMT is characterised by its photodetection efficiency and by the gain of the phototubes. Before associating sets of 4 MAPMTs into EC, the MAPMTs are sorted according their gain to get EC with MAPMT with close gain for the same HV (see [9]). For this, the gain are initially measured with sensitive, commercial multi-channels charge converters (QDC) for a gain, being a factor three above its nominal value, for a HV around -1100 V. Once the EC are assembled, the gain and the detection efficiency for each channels are measured with the ASICs at the nominal HV at -900 V. This operation is called the calibration. Both types of measurements are done with by illuminating the photocathode with a LED (monitored with a NIST-photodiode). The MAPMTs operates in single photoelectron mode [8] to measure the single photoelectron spectrum for each of the 2304 pixels of the instrument camera. This procedure allows to determine the exact high voltage to apply to the MAPMTs photocathodes of each EC Units.

### 4.3 The ASIC settings

The ASICs measure the single photoelectron spectra at nominal high voltage for each of the channels by performing S-curve (by performing series of runs by ramping the discriminator voltage). Because the relative gain of the channels inside an EC-Unit differs slightly from one-another, the ASICs allow balancing the discrepancies between the channels. This done once the PDM is mounted and each MAPMT is associated to an ASIC. Then the nominal discriminator threshold at 1/3 of a photoelectron to apply to each ASIC is established.

### 4.4 The Trigger tests

Once the PDM is mounted, including the PDMB, the L1 trigger algorithm performance is checked by illuminating the Focal Surface by the light spot moving closely to speed-of-light, generated by an "old" persistent-screen scope.

## 4.5 The Instrument tests

The final tests will be performed after the integration of all subsystems inside the instrument. A check of the correct final position of the lenses as well as that of the Focal Surface will be done by lighting up the first lens by a parallel UV beam along the optical axis. The size of the focused point on the Focal surface will be minimised by finely adjusting the position of the PDM at the sub-millimetre scale. At the end of the integration and at launch site, basic health tests on the electronics will be performed by illuminating uniformly directly the Focal Surface or the first lens by a LED-controlled, in single photon mode, as described in [8].

## 5 Operation and Analysis

During the balloon flight operation, the instrument will be controlled from ground by an operator using a control program [10] interfaced to the TC/TM system (Telecommand and Telemetry) NOSYCA of CNES. At a given altitude reached by the balloon, a command will be issued to turn on the instrument. The HK system will turn on one by one each of the subsystems while the monitoring parameter will be downloaded at ground. When every parameters looks perfect, after having chosen the convenient configuration parameters for the ASICs and the Triggers, the balloon operator can launch the DAQ program running on the CPU. He will control basic run parameters, namely the background rate calculated by the PDMB. Conventionally the thresholds auto-adapt to the required L1-L2 rates unless the operator forces another mode of trigger settings. At any moment, the operator can shut down the instrument. This will be done when the balloon descent will be activated.

## 6 Conclusion

A reduced scaled version of the future space telescope JEM-EUSO, but with similar instrumentation, is being built to serve as a pathfinder embarked in the gondola of a stratospheric balloon. EUSO-Balloon is by itself a complete autonomous instrument capable to perform the same kinds of measurements as JEM-EUSO, namely the photo detection, the analog and digital electronics involving the signal measurements, digitisation and the trigger, implemented in the developed ASICs and FPGA. Also, a Data Processing system has been developed including the data acquisition and the instrument monitoring. This telescope will be operational for CNES balloon campaigns next year.

**Acknowledgment:** This work was strongly, technically as well as financially supported by CNES and the JEM-EUSO collaboration.

## References

- [1] J.H. Adams Jr. *et al.* - JEM-EUSO Collaboration, *Astroparticle Physics* 44 (2013) 76-90  
<http://dx.doi.org/10.1016/j.astropartphys.2013.01.008>
- [2] P. von Ballmoos *et al.* - EUSO-BALLOON: a pathfinder for observing UHECR's from space, this proceedings, paper 1171,
- [3] T. Mernik *et al.* ESAF-Simulation of the EUSO-Balloon, this proceedings, paper 875,
- [4] Manufacturing of the TA-EUSO and EUSO-Balloon lenses, this proceedings, paper 1040,
- [5] P. Barrillon *et al.*, The Electronics of the EUSO-Balloon UV camera, this proceedings, paper 765,

- 
- [6] H. Miyamoto *et al.*, Performance of the SPACIROC front-end ASIC for JEM-EUSO, this proceedings, paper 1089,
  - [7] J. Bayer *et al.*, Second level trigger and Cluster Control Board for the JEM-EUSO mission, this proceedings, paper 432,
  - [8] P. Gorodetzky *et al.*, Absolute calibrations of JEM-EUSO, this proceedings, paper 858,
  - [9] C. Blaksley, Photomultiplier Tube Sorting for JEM-EUSO and EUSO-Balloon, this proceedings, paper 628,
  - [10] L.W. Piotrowski *et al.*, On-line and off-line data analysis for the TA-EUSO and BALLOON-EUSO experiments, this proceedings, paper 713,